Combination of classic geological/geophysical data analysis and machine learning: brownfield sweet spots case study of the middle Jurassic Formation in Western Kazakhstan

Authors: Natalia Osintseva[1], Dmitry Danko [1], Ivan Priezzhev [1], Kurmangazy Iskaziyev[2], Valery Ryzhkov [1]*
[1]Gubkin University, [2]JSC KazMunaiGas Exploration Production

Summary

At present time, many large oil and gas fields, discovered back in the 60-70s are at a late stage of development (brownfields). For this reason, there is an urgent issue of searching for the "missed" sweet spots. Our target is a multilayer oil and gas field in Western Kazakhstan, which is unique in reserves. More than 5000 wells have been drilled at this field and provided sufficient information for a detailed study of reservoir rocks in Middle Jurassic deposits. Using data obtained for one productive layer we present the methodology and results of identifying of the prospective objects for further exploitation of the target brownfield.

Introduction

The studied field is located within the Zhetybai-Uzen step of Western Kazakhstan and is confined to a large anticlinal fold. Gas fields were discovered in Cretaceous sedimentary rocks, while oil fields were found in Jurassic sedimentary rocks with gas caps and individual gas fields. In Jurassic sediments with a total thickness of about 1200 m, 13 productive intervals (numbered from top to bottom) stand out which are characterized by a strong lithological heterogeneity. The effective thickness of sand formations varies from less than a meter to 23 m, and only in the 12th productive interval reaches 47 m.

During the Jurassic time, at least two regional breaks in sedimentation are observed and reflected in different geometry and thickness of the sand bodies formed at different sea levels. For example, the 12th productive interval was formed during low standing of the sea level. Therefore, the sandy deposits of this layer are mainly represented by sediments of braided rivers with rather large thicknesses. Fields of the transgressive system tract are confined to the 11th productive interval and are quite thin due to the rapid rise in the sea level. Sand deposits formed during highstand of sea-level (from 8 to 10 productive intervals) in most cases are confined to meandering and anastomosing river systems and are characterized by small thicknesses. The second sequence boundary was revealed within the 7th productive interval and is represented by an incised valley on a part of the study area. The lowstand systems tract includes sediments from 3^{d} to 7th productive intervals and is characterized by a high content of sand material. The transgressive system tract is distinguished in the 1st and 2nd productive interval. The sand deposits of this system tract are characterized by a limited distribution over the area and are confined to coastal deposits and river systems.

In the study area we expect that the lithological traps could be formed in the sediments of the transgressive and high system tracts. Therefore, we chose the 1st productive interval for our analysis.

The analyzed interval is represented by continental, transitional, and shallow-marine facies. The section consists of interbedded sandy, siltstone, and clay deposits; interlayers of coal are encountered. The total thickness of the studied formation varies from 40 to 55 m. The result of core data analysis showed that the average reservoir porosity is equal to 26-27%. The carbonate-clay deposits of the Upper Jurassic are the caprock. Five interlayers (A, B, C, D, E) are identified inside the 1st productive interval.

Methodology

At the initial step of the research, sedimentation conditions of core data were analyzed with the identification of the main facies. Then, based on the classification of well log data for all 5000 wells, the distribution of well log facies (using self-potential and the gamma ray logs) have been identified. (Serra, 1975; Muromtsev, 1984). To classify well log curves in the analyzed interval, we used a well-known algorithm based on Kohonen neural networks (Kohonen, 1995). The main feature of the Kohonen classification algorithm is not only grouping similar objects into separate classes, but also ranking (sorting) these classes by the degree of similarity of typical (generalized) objects assigned to these classes. This feature allows us to perform visualization of the close classes using close color shades. In this work we used the three-dimensional Kohonen neural networks (Priezzhev et al, 2019). To visualize similar classes for a three-index space, RGB (red-green-blue) color mixing technology for individual indexes have been used. As shown earlier (Priezzhev et al, 2019), the application of a three-index space allows us to get the higher accuracy multidimensional relationship of the objects (well log curves, in our case) in comparison with the two-index and one-index Kohonen classification methods.

To determine the boundaries of studied objects and the sedimental sequences we used the results of the seismic waveforms classification, spectral decomposition, coherence, porosity and NTG (net-to-gross) volumes (Figure 1).

10.1190/segam2020-3425384.1

Porosity cube was calculated using extended elastic impedance technology (Whitcombe et. al., 2002) and NTG volume was obtained from pre-stack AVO/AVA seismic inversion result with applying the Vernik's equation (Vernik, 2002).

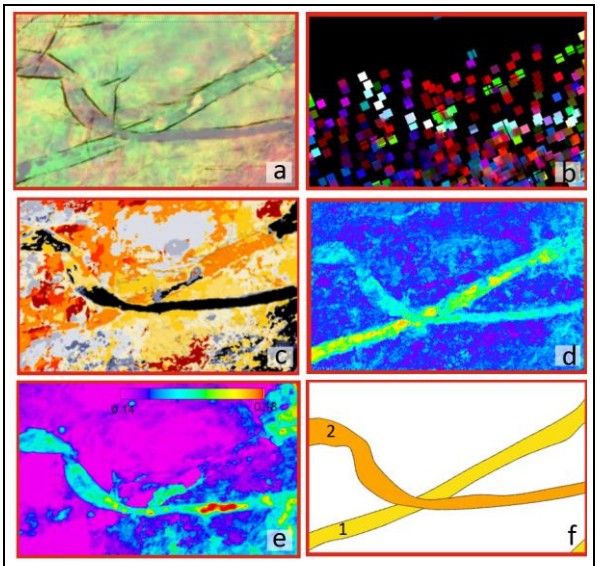

Figure 1: An example of the definition of objects contours and determination of the priority of their formation using the following data sets : a) spectral decomposition with coherence overlaying, b) well loging facies c) seismic facies d) net reservoir thickness map for the entire interval, e) slice of the porosity cube (for geological body 2), f) distinguished geological bodies and the sequence of their formation

At the final step, the reservoir thickness was predicted by the Kohonen neural networks using well log data, porosity and NTG volumes as input data.

Brownfield "sweet spot" analysis

According to the interpretation of core data from the 1st productive interval, one regressive-transgressive cycle is distinguished and shown in Figure 2.

Figure 3 illustrates the change in facies from the shallow marine/lagoon to continental, and then again to shallow marine/lagoon facies. Figure 3-f shows the photograph of the mudstone (from depth of 1105,5 m) that formed in shallow marine/lagoon sedimentary environment with a calm hydrodynamic setting. At a depth 1099 m there are layers that consist of whole and fragments of marine organisms shells, which indicates a more active hydrodynamic setting (Figure 3, e). Further, along the section at a depth of 1084 m,

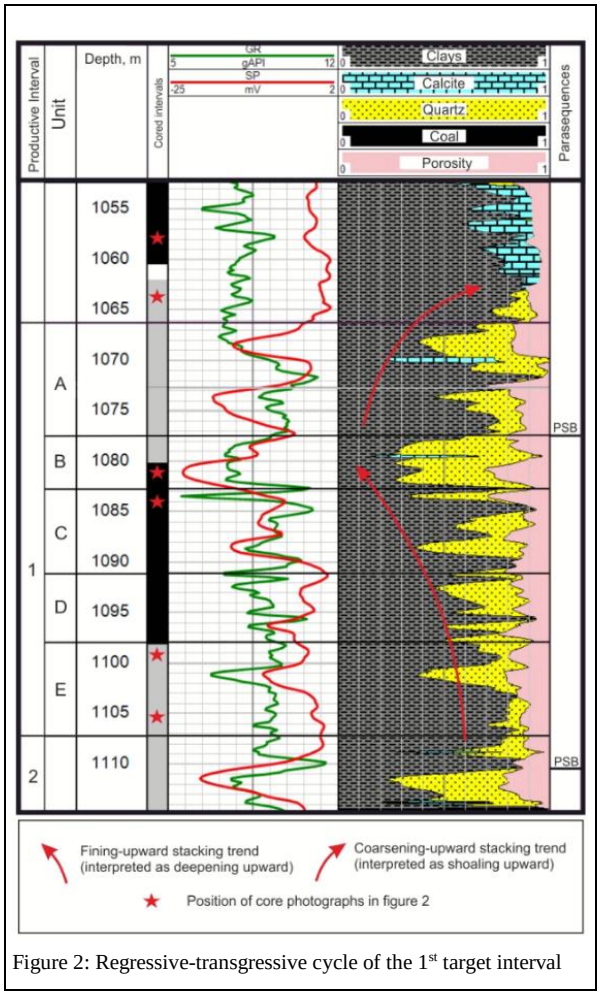

Figure 2: Regressive-transgressive cycle of the 1st target interval

one can see the traces of plant roots made by carbonaceous matter (Figure 3, d), traces of paleosol and interbeds of coal indicate a change to the continental depositional environment. At a depth of 1082 m there are sandy beds with oblique stratification (Figure 3, c) which are interpreted as sediments of a river system with a meandering channel. Higher in the geological section, sandstone and clay deposits with flaser and wavy bedding interlamination are distinguished (Figure 3, b), the formation of which took place in coastal settings. The entire section is overlain by clay deposits with inclusions of carbonate nodules/interlayers formed in shelf/lagoon environments (Figure 3, a).

The calculation of well log facies for each interlayer (A-E) made it possible to establish the sequence of formation

10.1190/segam2020-3425384.1

Combination of classic geological/geophysical data analysis and machine learning: brownfield sweet spots case study of the middle Jurassic Formation in Western Kazakhstan

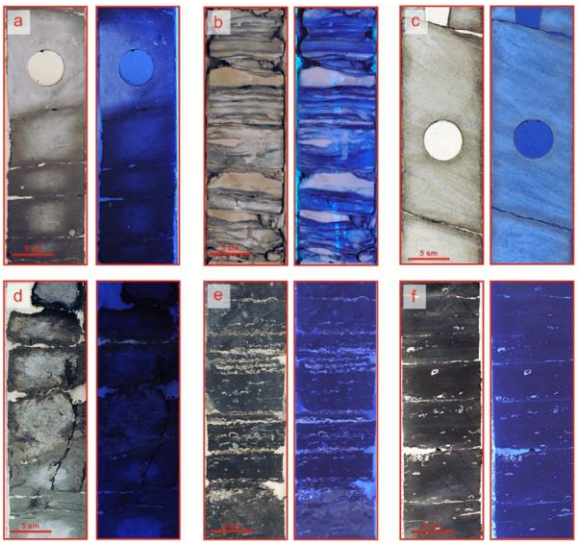

Figure 3: Core photographs in daylight and ultraviolet light. The depth of sampling is shown in Figure 1. a) clay deposits with a carbonate layer (depth of 1057,5 m), b) interbedded sand and clay layers - wavy layering (depth of 1064 m), c) cross bedded sandstone (depth of 1082 m), d) organic-rich rooting muds forming floodplain deposits (depth of 1084 m), e) laminated mudstone and bioclastic limestone depth of 1099 m, f) mudstone with single carbonate shells (depth of 1105,5 m)

of the selected sand bodies (Figure 4). In order to geometrize bodies using seismic data sets (spectral decomposition, coherence, porosity and NTG cubes), a series of stratal slices were generated in a 2 ms interval. By viewing of these stratal slices in different order we have recognized a boundary of every single sand body. The seismic geomorphology of sand

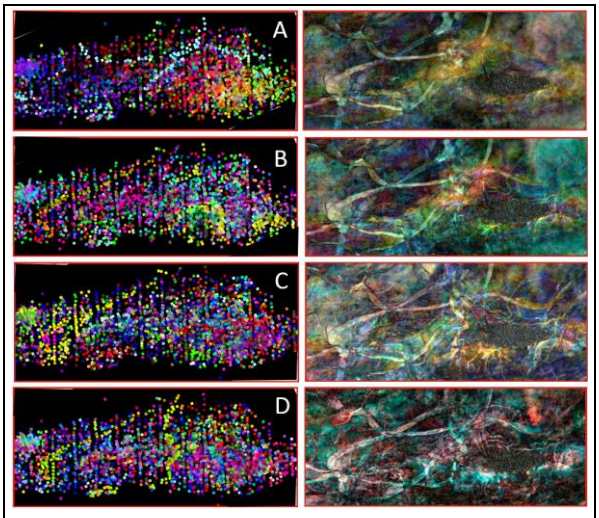

Figure 4: Well log facies for interlayers A, B, C, D (left) and spectral decomposition for corresponding intervals (right)

bodies helped to determine the supposed sedimentation conditions (Posamentier, 2007; Zeng, 2015).

Resulting facies maps were constructed that illustrate the change in coastline regression from east to west (relative time 1–4), and coast line transgression (relative time 5 and 6 on Figure 5). We interpreted isolated sand bodies as delta systems, estuaries, barrier-island coasts, meandering and anastomosing river systems.

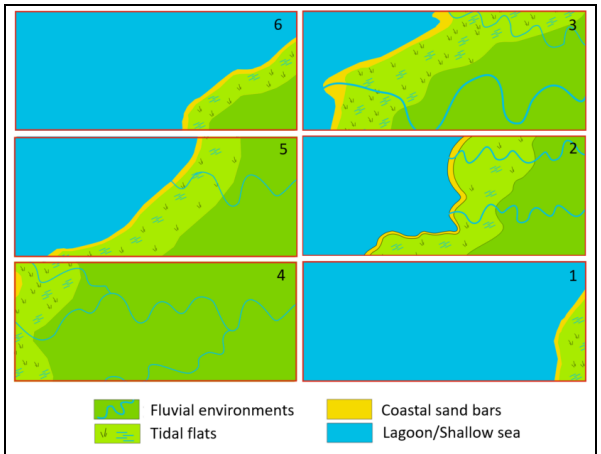

Figure 5: Sedimentation model (numbers from 1 to 6 indicate the reletive age)

Since the isolated sand bodies formed at different geological times, it is expected that they will be partially or completely isolated from each other and can form lithological traps. Evidently, due to this factor a different level of water-oil contact is distinguished for the studied productive interval.

Based on the analysis of all available data, a number of prospective objects have been identified. Two of which are illustrated in Figure 6. These objects are interpreted as anastomizing river systems which are laterally replaced by mudstone floodplain deposits. Mudstone transgressive stratum overlies these sandy bodies. Therefore, we assume, that the lithological traps may be associated with the isolated selected objects.

Conclusions

It is demonstrated that it is possible to find missing objects for future development in a well-drilled oilfield characterized by strong lithological heterogeneity of sediments.

The proposed methodology for combining classical approaches to the interpretation of multiscale geological and

10.1190/segam2020-3425384.1

geophysical data and machine learning techniques can be useful for sweet spot analysis on brownfields.

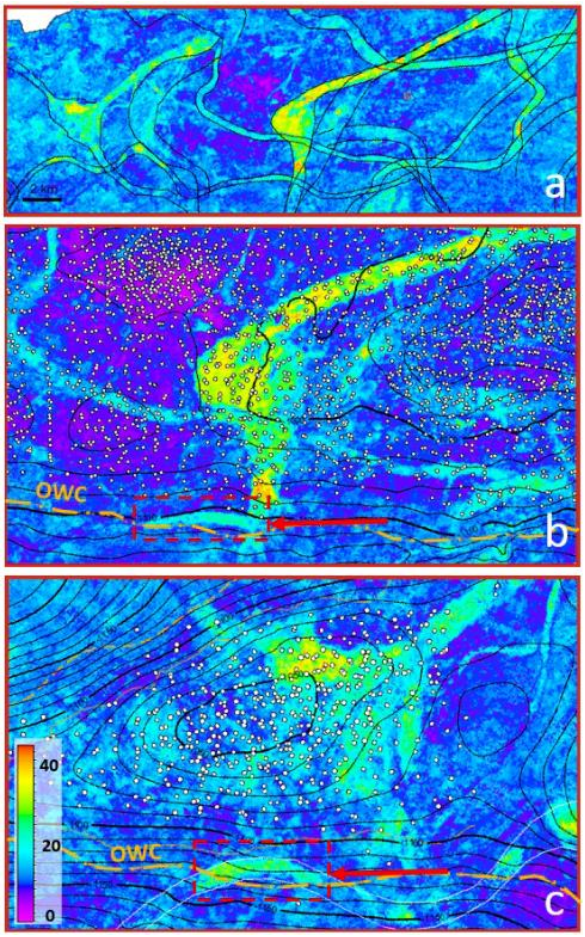

Figure 6: a) Net reservoir thickness map for the target interval with contoured sand bodies, b) and c) Zoomed fragments with perspective objects (enclosed in frames). White dots show the wells location

Acknowledgments

The work was carried out at Department of exploration geophysics of Gubkin University. The authors gratefully acknowledge JSC KazMunaiGas Exploration Production for the data provided. Also we thank CGG and Schlumberger for G&G software support.

10.1190/segam2020-3425384.1

REFERENCES

Kohonen, T., 1995, Self-organizing maps: Springer-Verlag, New York, Inc.

Muromtsev, V. S., 1984, Electrometric geology of sand bodies — Lithological traps of oil and gas: Nedra (Rus).

Posamentier, H. W., J. A. Davies, J. A. Cartwright, and L. Wood, 2007, Seismic Geomorphology — An overview, in R. J. Davies, H. W. Posamentier, L. J. Wood, and J. A. Cartwright, 2007, Seismic Geomorphology: applications to hydrocarbon exploration and production: Geological Society Special Publication No. 277, 1–14.

Priezzhev, I. I., P. C. H. Veeken, S. V. Egorov, A. N. Nikiforov, and U. Strecker, 2019, Seismic waveform classification based on Kohonen 3D neural networks with RGB visualization: First Break, **37**, 37–43.

Serra, O., and L. Sulpice, 1975, Sedimentological analysis of shale-sand series from well logs: Presented at the SPWLA 16th Annual Logging Symposium.

Vernik, L., D. Fisher, and S. Bahret, 2002, Estimation of net-to-gross from P and S impedance in deepwater turbidites: The Leading Edge, **21**, 380–387, doi: https://doi.org/10.1190/1.1471602.

Whitcombe, D. N., P. A. Connolly, R. L. Reagan, and T. C. Redshaw, 2002, Extended elastic impedance for and lithology prediction: Geophysics, **67**, 63–67, doi: https://doi.org/10.1190/1.1451337.

Zeng, H., 2015, Predicting geometry and stacking pattern of thin beds by interpreting geomorphology and waveforms using sequential stratal-slices in the Wheeler domain: Interpretation, **3**, no. 3, SS49–SS64, doi: https://doi.org/10.1190/INT-2014-0181.1.

10.1190/segam2020-3425384.1